NASA/TM—2011-217408

Effect of Upper-Cycle Temperature on the Load-Biased, Strain-Temperature Response of NiTi

Santo Padula, II, Ronald Noebe, and Glen Bigelow
Glenn Research Center, Cleveland, Ohio

Shipeng Qiu and Raj Vaidyanathan
University of Central Florida, Orlando, Florida

Darrell Gaydosh
Ohio Aerospace Institute, Brook Park, Ohio

Anita Garg
University of Toledo, Toledo, Ohio

December 2011

NASA STI Program . . . in Profile

Since its founding, NASA has been dedicated to the advancement of aeronautics and space science. The NASA Scientific and Technical Information (STI) program plays a key part in helping NASA maintain this important role.

The NASA STI Program operates under the auspices of the Agency Chief Information Officer. It collects, organizes, provides for archiving, and disseminates NASA's STI. The NASA STI program provides access to the NASA Aeronautics and Space Database and its public interface, the NASA Technical Reports Server, thus providing one of the largest collections of aeronautical and space science STI in the world. Results are published in both non-NASA channels and by NASA in the NASA STI Report Series, which includes the following report types:

- TECHNICAL PUBLICATION. Reports of completed research or a major significant phase of research that present the results of NASA programs and include extensive data or theoretical analysis. Includes compilations of significant scientific and technical data and information deemed to be of continuing reference value. NASA counterpart of peer-reviewed formal professional papers but has less stringent limitations on manuscript length and extent of graphic presentations.

- TECHNICAL MEMORANDUM. Scientific and technical findings that are preliminary or of specialized interest, e.g., quick release reports, working papers, and bibliographies that contain minimal annotation. Does not contain extensive analysis.

- CONTRACTOR REPORT. Scientific and technical findings by NASA-sponsored contractors and grantees.

- CONFERENCE PUBLICATION. Collected papers from scientific and technical conferences, symposia, seminars, or other meetings sponsored or cosponsored by NASA.

- SPECIAL PUBLICATION. Scientific, technical, or historical information from NASA programs, projects, and missions, often concerned with subjects having substantial public interest.

- TECHNICAL TRANSLATION. English-language translations of foreign scientific and technical material pertinent to NASA's mission.

Specialized services also include creating custom thesauri, building customized databases, organizing and publishing research results.

For more information about the NASA STI program, see the following:

- Access the NASA STI program home page at *http://www.sti.nasa.gov*

- E-mail your question via the Internet to *help@sti.nasa.gov*

- Fax your question to the NASA STI Help Desk at 443–757–5803

- Telephone the NASA STI Help Desk at 443–757–5802

- Write to:
  NASA Center for AeroSpace Information (CASI)
  7115 Standard Drive
  Hanover, MD 21076–1320

Effect of Upper-Cycle Temperature on the Load-Biased, Strain-Temperature Response of NiTi

Santo Padula, II, Ronald Noebe, and Glen Bigelow
Glenn Research Center, Cleveland, Ohio

Shipeng Qiu and Raj Vaidyanathan
University of Central Florida, Orlando, Florida

Darrell Gaydosh
Ohio Aerospace Institute, Brook Park, Ohio

Anita Garg
University of Toledo, Toledo, Ohio

Acknowledgments

Level of Review: This material has been technically reviewed by technical management.

Available from

NASA Center for Aerospace Information
7115 Standard Drive
Hanover, MD 21076–1320

National Technical Information Service
5301 Shawnee Road
Alexandria, VA 22312

Available electronically at http://www.sti.nasa.gov

Effect of Upper-Cycle Temperature on the Load-Biased, Strain-Temperature Response of NiTi

Santo Padula, II, Ronald Noebe, and Glen Bigelow
National Aeronautics and Space Administration
Glenn Research Center
Cleveland, Ohio 44135

Shipeng Qiu and Raj Vaidyanathan
University of Central Florida
Orlando, Florida 32816

Darrell Gaydosh
Ohio Aerospace Institute
Brook Park, Ohio 44142

Anita Garg
University of Toledo
Toledo, Ohio 43606

Abstract

Over the past decade, interest in shape memory alloy based actuators has increased as the primary benefits of these solid-state devices have become more apparent. However, much is still unknown about the characteristic behavior of these materials when used in actuator applications. Recently we have shown [1] that the maximum temperature reached during thermal cycling under isobaric conditions could significantly affect the observed mechanical response of NiTi (55 wt% Ni), especially the amount of transformation strain available for actuation and thus work output. The investigation we report here extends that original work to ascertain whether further increases in the upper-cycle temperature would produce additional changes in the work output of the material, which has a stress-free austenite finish temperature of 113 ^{o}C, and to determine the optimum cyclic conditions. Thus, isobaric, thermal-cycle experiments were conducted on the aforementioned alloy at various stresses from 50-300 MPa using upper-cycle temperatures of 165, 200, 230, 260, 290, 320 and 350 ^{o}C. The data indicated that the amount of applied stress influenced the transformation strain, as would be expected. However, the maximum temperature reached during the thermal excursion also plays an equally significant role in determining the transformation strain, with the maximum transformation strain observed during thermal cycling to 290 ^{o}C. *In situ* neutron diffraction at stress and temperature showed that the differences in transformation strain were mostly related to changes in martensite texture when cycling to different upper-cycle temperatures. Hence, understanding this effect is important to optimizing the operation of SMA-based actuators and could lead to new methods for processing and training shape memory alloys for optimal performance.

I. Introduction

Shape memory alloys (SMAs) are slowly but steadily being viewed as a viable, solid-state replacement for hydraulic and pneumatic actuation systems. However, before serious inroads can be made, a better understanding of the macroscopic response of these unique materials, especially under constant-stress, thermal cycling conditions is necessary. To date, the majority of research has focused on the isothermal, superelastic properties of SMAs, as these properties are useful in bio-medical applications. However,

the isobaric, strain-temperature response of the material is more pertinent when dealing with actuation-based applications. Although many SMAs have been studied to ascertain transformation temperatures and shape recovery under stress-free conditions, a much smaller subset has been investigated to determine transformation strain or work output characteristics under bias-stress conditions. Among the materials that have been studied for their actuation characteristics, much of the work has focused on the effect of applied stress on the observed performance. Various authors have shown that increases in the applied stress not only affect the transformation strain [2-7], but also affect the transformation temperatures according to the Clausius-Clapeyron relationship [8, 9]. However, it has also been reported that the history of the applied stress can affect the level of dimensional stability observed [5, 10]. While the magnitude of the applied stress is extremely important in determining the actuator-specific characteristics of a given material, this work explores the role of upper-cycle temperature (UCT), the highest temperature reached during the thermal excursion, on the load-biased thermal-cyclic response of an SMA.

II. Procedures

A. Material

The material used in this study was a commercially available, binary NiTi alloy produced by Special Metals, New Hartford, New York, with a fully annealed ingot A_s temperature of 95 +/- 5 ^{o}C, henceforth designated as 55NiTi. In this case 55 refers to the wt% Ni in the alloy. In terms of at%, the stoichiometry of the alloy is $Ni_{49.9}Ti_{50.1}$, which is optimized for high transformation temperature. The material was delivered as 10mm diameter rods in the hot-rolled/hot-drawn and hot-straightened condition. DSC measurements on the as-received material using a heating/cooling rate of 10°C/min indicated stress-free transformation temperatures of 47, 75, 89 and 113 ^{o}C for the M_f, M_s, A_s and A_f, respectively. Cylindrical, uniform gage length tensile specimens having a diameter of 3.85 mm and a reduced gage length of 25.4 mm were machined from the hot-rolled stock.

B. Constant-Stress, Thermal-Cycle Testing (Load-biased)

Subsequent to thermal-cycle testing at constant load (also referred to as load-biased testing), two thermal cycles in the absence of any load were performed on the as-machined specimen prior to performing any other operation. The intent of these no-load thermal cycles was to relieve any internal stresses resulting from the machining operation. Once the no-load cycles were complete, the specimens were tested using a so-called "series" load-biased methodology, as described in the following.

A "series" load-biased, thermal-cycle test consisted of loading the stress-relieved specimen at room temperature, in the martensite state, to a predetermined stress at a strain rate of 1x10^{-4} s^{-1} using strain control. Once the desired stress level was achieved, the controller was switched into load control and the stress was held constant. The specimen was then thermally cycled from room temperature (RT) to the desired upper-cycle temperature and back for two complete thermal cycles. After completing the two thermal cycles, the controller was switched back to strain control and the same specimen was strained until the next higher stress level was achieved. Once the desired stress level was achieved, the control-mode was switched back to load control and the thermal cycling process was repeated. This process of loading in strain control followed by thermal cycling under constant stress was repeated until all desired stress levels were completed

using the same specimen (hence the notation "series" load-biased). Stress levels from 50-300 MPa (in 50 MPa increments) were assessed. To determine the effect of upper-cycle temperature on the observed load-biased, strain-temperature response, upper-cycle temperatures of 165, 200, 230, 260, 290, 320 and 350 ^{o}C were used. In all cases, only the second heating and cooling cycle for a given stress was used for analysis. This second heating and cooling cycle was chosen because of the nature of the processes involved in the response. When a stress is applied to the material or a change in the applied stress is made, significant changes in the martensite variant structure results during the first thermal cycle. Hence, the first cycle is not representative of subsequent cycles at a given stress and is therefore not used for analysis [1]. We refer to the aforementioned methodology as "series" to contrast it with a methodology wherein a different starting specimen is used for each combination of stress/temperature. Previous work has shown that results from the "series" testing methodology are comparable with results obtained from individual specimens when testing is limited to a few cycles (less than 10).

C. *In situ Neutron Diffraction*

In situ neutron diffraction measurements were performed in "time-of-flight" mode using the Spectrometer for MAterials Research at Temperature and Stress (SMARTS) at Los Alamos National Laboratory (LANL). Additional details of the neutron diffraction setup can be found in Ref. [11]. Due to the penetration depth of neutrons, any observed differences are representative of changes occurring throughout the bulk of the material, not merely surface measurements as would be the case if x-ray diffraction from a conventional source was utilized. Neutron diffraction measurements were conducted in an identical manner to the "series" load-biased experiments described previously with the only exception being that, at the extents of the temperature cycle (i.e., whenever the upper-cycle temperature was achieved or whenever the specimen reached room temperature), the specimens were held for 5 min before taking a measurement to allow for the temperature to equilibrate and 30 min were allowed to acquire neutron spectra. Both Rietveld and single peak analyses were used, following the methodology established previously for analyzing neutron diffraction spectra in NiTi alloys [12, 13], to obtain quantitative information on the micromechanical and microstructural evolution, e.g., lattice strains, phase volume fractions and texture, in the martensite as well as austenite phases that occurred during load-biased, thermal-cycling experiments.

D. *Determination of Transformation-Specific Properties*

The data presented in this paper was taken from the second cycle of the "load-biased", thermal-cycling experiment after each load change, and is in the form of the measured axial strain as a function of temperature during that thermal excursion (See Figure 1). This strain/temperature data is then used to determine all of the relevant properties for the transformation for a given stress/upper-cycle temperature combination.
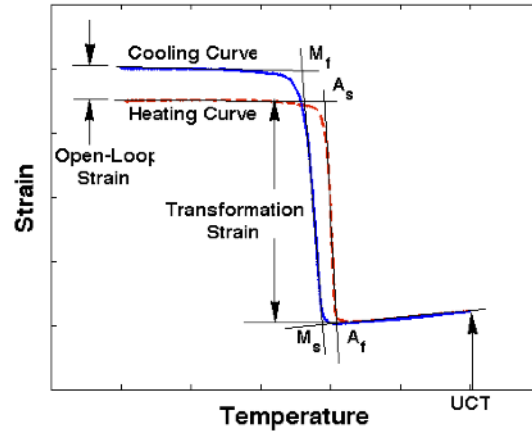
Figure 1: Properties relevant to a load-biased, thermal-cycle experiment where M_s, M_f, A_S and A_f are the martensite start, martensite finish, austenite start and austenite finish temperatures, respectively.

To determine transformation temperatures for the alloy, lines were fit through the three distinct linear sections of the strain-temperature data associated with the phase transformation. The temperatures where these lines intersect were taken to be the respective transformation temperatures. Similarly, the transformation strain was defined as the difference in strain measured where the lines intersect during the heating portion of the cycle. This convention was chosen because this is the most common mode of utilizing an SMA for actuation (recovering strain under a bias stress). Finally, the dimensional instability or "open-loop" strain was determined by measuring the difference in strain that developed from the beginning to the end of the thermal excursion and was taken to be the strain difference at room temperature. The aforementioned parameters are schematically shown in Figure 1 and were assessed to determine the dependency that each has with respect to both the applied stress and the upper-cycle temperature used in the experiment.

III. Results and Discussion

Although a working knowledge of the magnitudes of the various transformation-specific properties are extremely important to the successful utilization of SMAs, obtaining a better understanding of the functional dependency of these properties on the imposed conditions (namely, stress and temperature) is equally important. Once a mapping of the dependency of the various properties to either the stress and/or temperature has been accomplished, regions that provide the best overall material characteristics can be identified and used to optimize system performance. The information obtained by mapping these stress-temperature-property spaces can also guide work in other areas important to SMAs, such as training and processing. Consequently, a large portion of the stress-temperature-transformation property space was systematically investigated for binary NiTi in the hot-rolled condition. Although the material has not yet achieved a stabilized state by the end of the second load-biased thermal cycle, this condition incorporates the largest degree of microstructural evolution, which occurs during the first cooling portion of the cycle immediately after a change in stress has occurred, and can be used as a good gauge for the material's response to the applied conditions.

A. *Load-biased Response and Total Strain Evolution*

Figure 2a shows the development of strain that occurs during various portions of a series, load-biased thermal cycling experiment for a UCT of 200 °C. From the figure it can be seen that, as the specimen is loaded at room temperature, a small strain develops commensurate with the elastic and isothermal de-twinning response of the material (Stage 0-1). The presence of de-twinning at these low stresses is confirmed by the transient strain response discussed below during heating and is expected given the starting hot-worked condition of the alloy. It is also consistent with previous observations of de-twinning at very low stresses in NiTi (less than 66 MPa) [14]. At this point, the initial fixed stress is maintained and the specimen is thermally cycled between room temperature and a fixed upper-cycle temperature, in this case 200 °C. Upon heating, a small strain transient is observed as the de-twinned material reverts to the parent austenite structure (Stage 1-2). Once the upper-cycle temperature has been reached, the specimen is cooled back to room temperature, while still under load. During the forward transformation (Stage 2-3), a large strain transient is observed. This strain transient, as will be seen later, is in part due to preferred variant selection that occurs when cooling from the parent austenite under an applied stress. We note that these transients are very important in correlating stability with the internal stress state in shape memory alloys and is the subject of an ongoing study. Also important to note is that this same transient phenomenon occurs over the first thermal cycle any time the specimen is loaded to a new stress level (See Stages 1-3, 6-8, etc.). Since the transient nature of this response makes it difficult to determine transformation specific properties like transformation strain, open-loop strain and transformation temperatures, the second cycle of the load-biased experiments were used to characterize the material. Figure 2b shows only the 2nd cycle response for the material shown in Figure 2a, from which all basic shape memory properties are extracted using the methodology defined in Figure 1. Using the second cycle not only allows for good property determination but also provides the earliest condition wherein the greatest amount of evolutionary differences imparted by the application of stress and temperature can be observed.
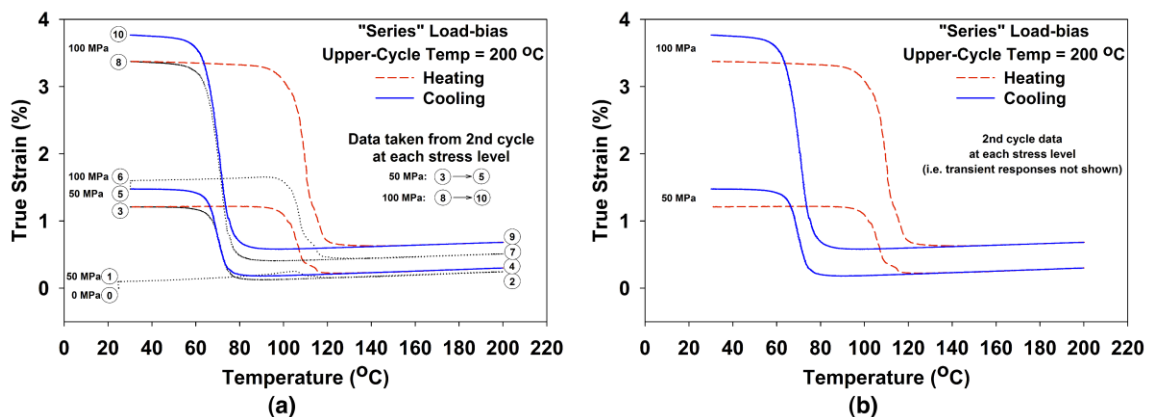

Figure 2: (a) Strain development in 55NiTi showing all cycles during a series, load-bias thermal cycling experiment with a UCT of 200 °C. The red (dashed) and blue (solid) portions of the curve indicate the heating and cooling portions of the load-bias cycle during the second cycle at various stresses. The black lines represent the initial transient response after a stress change. (b) Only data from the second cycle is shown for clarity, consistent with the way the data is presented in Figure 3.

From Figure 3, it is clear that both the stress and the upper-cycle temperature have an impact on the amount of strain and the shift in transformation temperatures that occur in the system. The underlying reasons for this observation will be discussed in detail in subsequent sections; the point that must be made here is that *both* stress and upper-cycle temperature have an effect on the observed responses. As the applied stress is increased, the material evolves such that a greater level of strain is achieved. This is apparent by looking at any of the individual series plots presented in Figure 3. In fact, the strain that results by the end of the load-biased series test can be quite large, on the order of 8% for the martensite state when an upper-cycle temperature of 165 ^{o}C is used. However, performing the identical load-biased series experiment with the UCT being the only parameter that is changed can produce dramatic increases in the absolute strains that are observed, reaching strains on the order of 20% in the martensite when a UCT of 350 ^{o}C is used. Thus, overall changes in strain evolution are also dramatically effected by changes in the upper-cycle temperature.
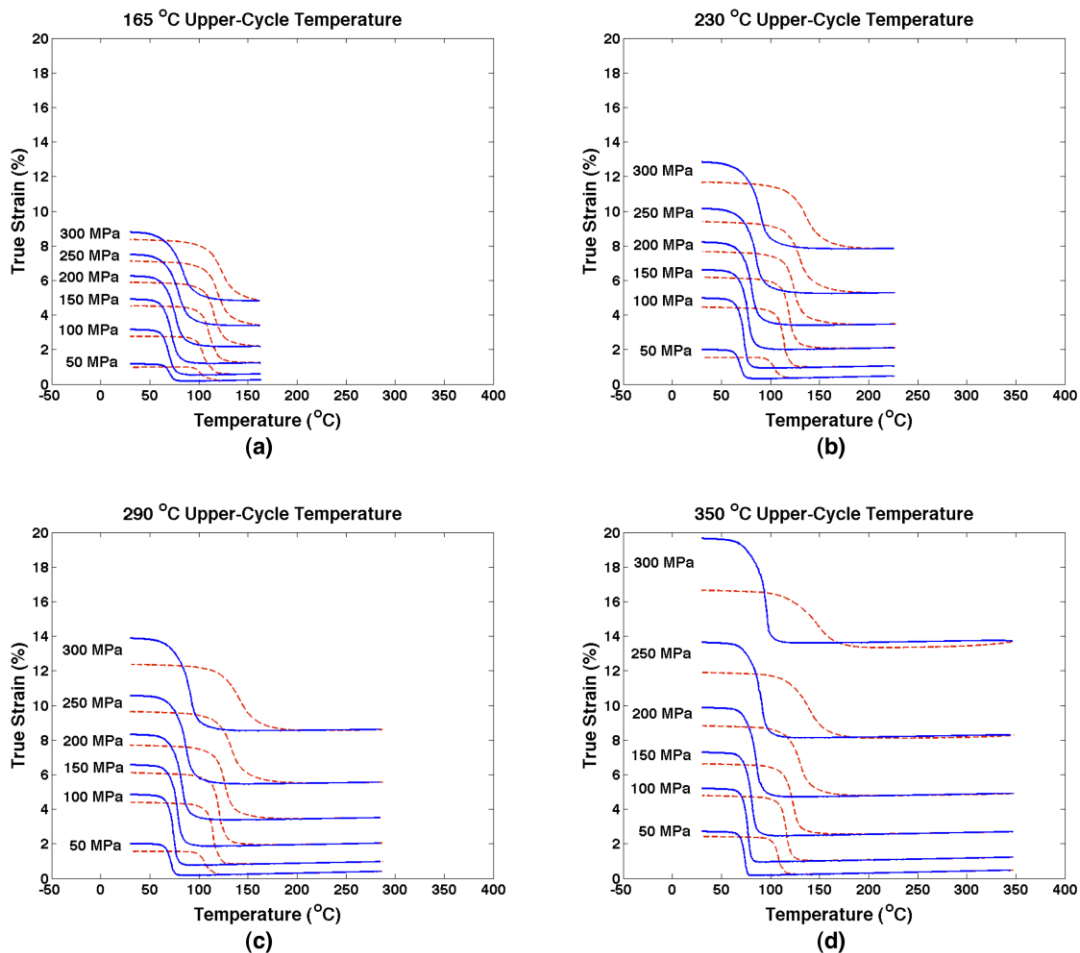

Figure 3: Second cycle data for the series, load-bias experiments conducted using upper-cycle temperatures of (a) 165 ^{o}C, (b) 230 ^{o}C, (c) 290 ^{o}C and (d) 350 ^{o}C, showing the difference in strain evolution that occurs as the upper-cycle temperature is changed.

It is also important to note that at upper-cycle temperatures above 200 ^{o}C, the majority of the curves exhibit a segment in the strain-temperature response where the strain change is

unaffected by temperature increases beyond the apparent A_f temperature (except for thermal expansion strains). This, plus the observation that the heating and cooling portions of the curve are superimposed in this region, indicates that inelastic deformation mechanisms such as plasticity, if occurring in the austenite phase, do not clearly manifest in these curves.

B. *Transformation Temperatures*

In general, most studies dealing with SMAs in one way or another report on the transformation temperatures of the material under investigation. Often times, as previously stated, only the "no-load" or "stress-free" temperatures are denoted. In other cases, the shift in the transformation temperatures due to the presence of stress has been reported [8, 9] and is commonly explained by the Clausius-Clapeyron relationship.
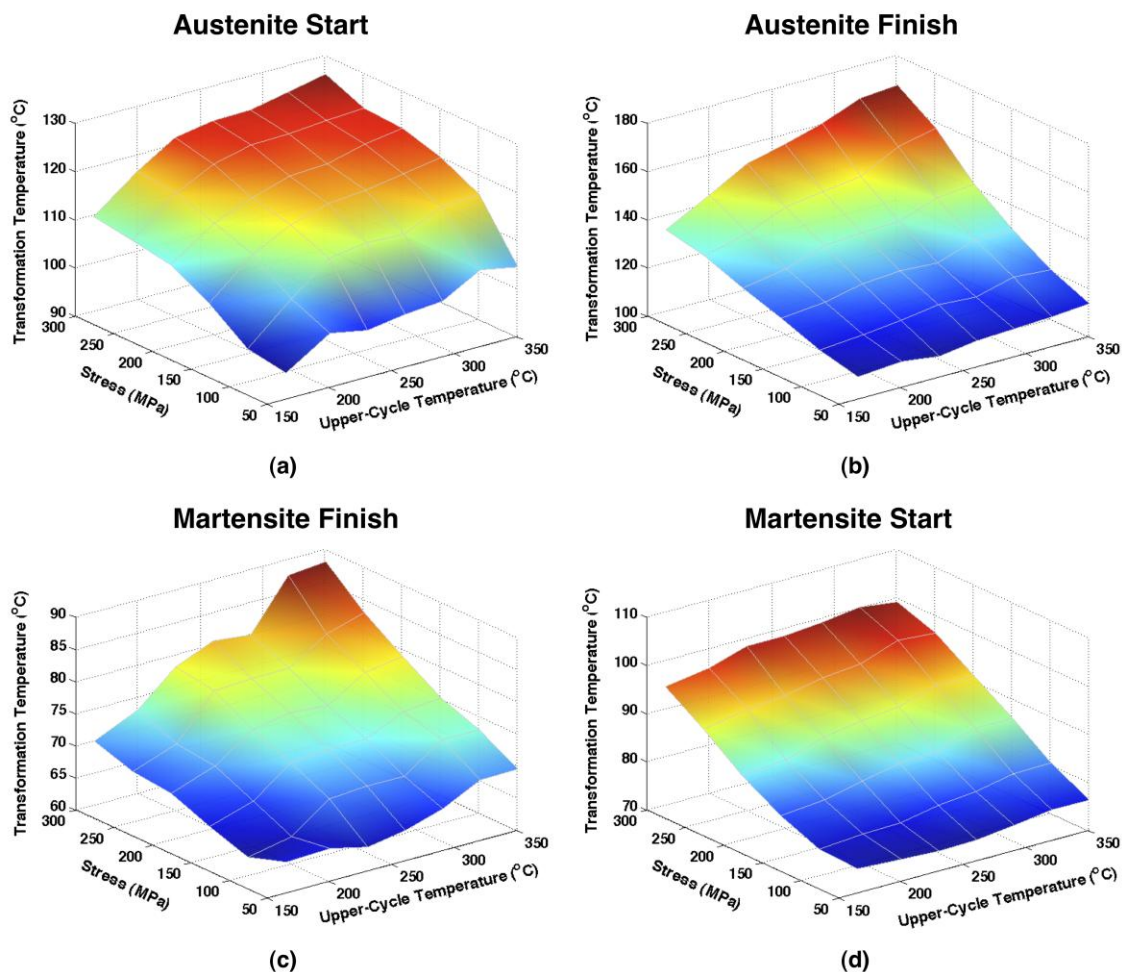

Figure 4: Effect of applied stress and upper-cycle temperature on the transformation temperatures for hot-rolled, binary NiTi.

Although the application of stress does have an effect on the measured transformation temperatures, it is not the only factor that influences these temperatures. As can be seen

in Figure 4, changing the upper-cycle temperature can also impact the measured transformation temperatures. In some cases, this effect can be as important as the effect associated with the externally applied stress indicating that the upper-cycle temperature must not be neglected when analyzing and comparing results. Even though the Clausius-Clapeyron relationship can be readily utilized with reasonable agreement in a number of circumstances, the data in Figure 4 indicates that the generalized form of this relationship cannot account for all of the factors that govern the true response of the material. As can be seen in Figure 4, both the austenite start (A_s) and martensite start (M_f) show a non-linear response with stress and upper-cycle temperature (See also Figure 5). It is seen that the transformation temperatures are shifted to higher values merely by increasing the UCT. This observation can clearly be seen in Figure 5 where the A_s temperature is shown to be shifted by as much as 20 ^{o}C or more by increasing the UCT. In general, increasing the UCT would not ordinarily have been thought to have a dramatic effect since the transformation would have been assumed to have already completed at the austenite finish (A_f) temperature. This clearly indicates that changes occurring within the material as a result of heating the sample under stress to temperatures beyond A_f during the thermal excursion play a significant role in determining the transformation character of the system. This effect is as quantitatively significant on the observed transformation temperatures as the effect of stress, a result that is clearly evident from the data presented in Figure 5.
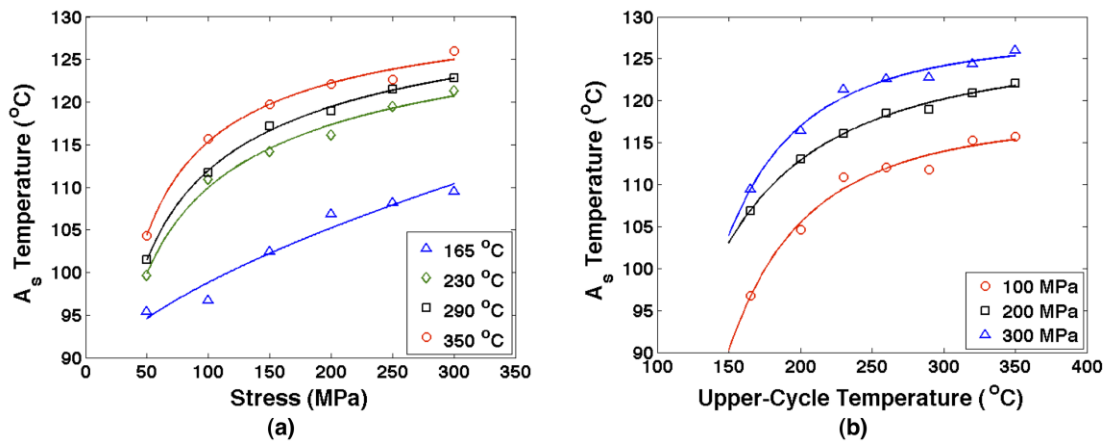

Figure 5: (a) Temperature and (b) Stress slices through the A_s temperature surface showing that the effect of upper-cycle temperature is as important as the effect of stress on determining the observed transformation temperature.

C. Recoverable Transformation Strain and Dimensional Instability (Open-Loop Strain)

When used as a solid-state actuator, SMAs must be able to do work against an externally imposed stress. Since the normalized work that a given material is capable of performing is directly dependant on the recoverable transformation strain at a given stress, it becomes increasingly important to establish the limits of a given material with regard to actuator-specific properties such as the transformation and open-loop strains.

Although it is commonly understood that both the transformation strain and open-loop strain, which is the component of strain not recovered during the thermal excursion, are related to the bias-stress, we are not aware of any literature regarding the dependence of these strains on changes in the temperature used during thermal cycling. As was seen in the assessment of the transformation temperatures, both the applied stress and the upper-cycle temperature had an influence on the measured response. It is therefore expected that both the stress and upper-cycle temperature also play a role in governing other actuator specific properties like transformation strain and dimensional instability (in this case as measured by the open-loop strain). Figure 6 shows the functional nature of these two properties for binary NiTi in the hot-rolled condition. As can be seen, the transformation and open-loop strains have a strong dependence on both the bias-stress and upper-cycle temperature.
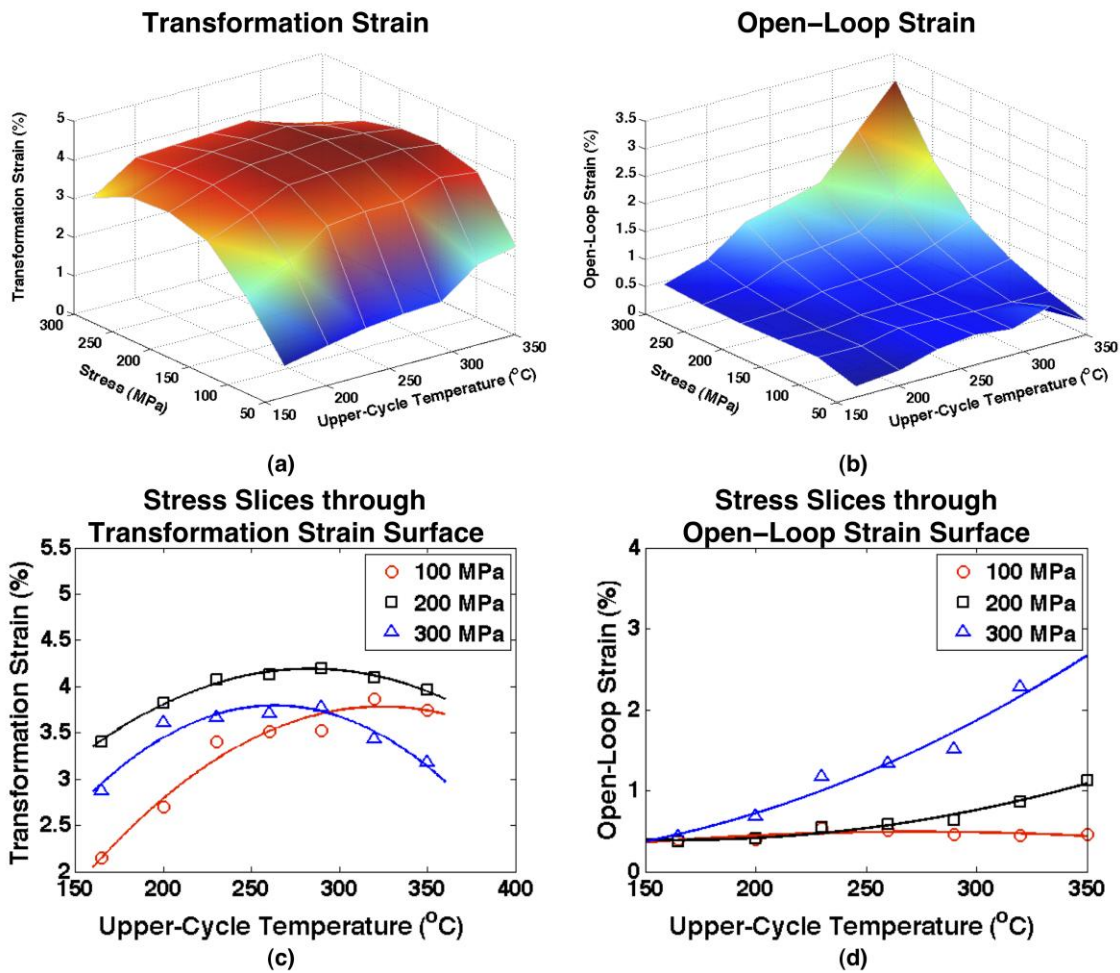

Figure 6: Dependence of the (a) transformation strain and (b) open-loop strain for hot-rolled, binary NiTi as a function of applied stress and upper-cycle temperature. Iso-stress slices taken through the (c) transformation strain surface and (d) open-loop strain surface at different stress levels clearly showing the effect of UCT on the observed quantities.

The results shown in Figure 6 indicate that a particular level of transformation strain (or open-loop strain) can be obtained by operating at more than one point in stress/temperature space. Thus, it is important to determine whether these commonalities in the response are produced because the underlying microstructures are the same or whether differences within the microstructure are independently resulting in similar shape memory responses. Such an understanding is important since other properties such as fatigue life may be deleteriously impacted even though properties like transformation strain and dimensional stability are similar for different stress-temperature combinations.

D. In situ Neutron Diffraction

D.1 Martensite Evolution

In situ neutron diffraction experiments were performed at selected load-biased thermal cycling conditions to investigate the effect of stress and upper-cycle temperature on underlying microstructural changes that might help explain the shape memory response of NiTi. Figure 7 are sections of normalized neutron diffraction spectra recorded at room temperature, showing the change in martensite texture with different UCTs and stress. The spectra shown here are from diffracting lattice planes parallel to the loading axis and were selected to track the texture evolution. Regardless of the external stress applied, with increasing UCT, the ratios of the intensities of the 100 martensite reflections to the intensities of the 011 martensite reflections increase. This favorable alignment of 100 martensite variants at the expense of 011 martensite variants relative to the loading direction is consistent with a (11-1) type I twinned structure [15]. The figure also shows that the magnitude of the applied stress has an impact on the orientation of variants formed during cycling under stress. Increases in the applied stress also tended to bias the system toward the alignment of 100 variants parallel to the loading direction, as is indicated by the larger 100/011 variant ratios. Note that the higher stresses and temperatures tend to converge to similar 100/011 ratios. This indicates similar underlying preferred martensite variant structures, i.e. the orientations of the martensite variants were similar. We note that the discussion presented here is based on representative single peak intensities in order to provide qualitative insight into the role of UCT and stress on the transformation and open-loop strains. A more complete and detailed analysis of the texture evolution that is consistent with the aforementioned observations from the 100 and 011 martensite reflections is presented in a companion article [16].

Figure 8 shows slices through the transformation strain and open-loop strain surfaces (taken from Figure 6) superimposed with the ratios of the intensities of the 100 martensite reflections to the intensities of the 011 martensite reflections from the neutron diffraction experiments. By presenting the data in this manner, a number of observations can be made. First, an almost factor of two increase in the transformation strain was observed for the 100 MPa condition, merely by increasing the upper-cycle temperature used during thermal cycling. This increase resulted because of the texture evolution that occurred with increasing upper-cycle temperature, as is indicated by the change in the peak intensity ratios. Second, increasing the stress from 100 to 200 MPa also had an impact on the texture of the resulting martensite, which in-turn affected the amount of transformation strain observed. However, further increases in the applied stress did not lead to even greater increases in transformation strain but rather lead to a lowering of the

strain recovery capability of the material, as exemplified by the 300 MPa condition that had similar second cycle 100 to 011 martensite peak intensity ratio but lower recoverable strain capability than was observed for other conditions. Neutron diffraction data was not available for the 300 MPa/320 °C condition since the sample broke before the data could be generated, but it would be assumed that the ratios of the intensity of the 100 martensite reflection to the intensity of the 011 martensite reflection would be similar, i.e., at a level near 1.32-1.34.
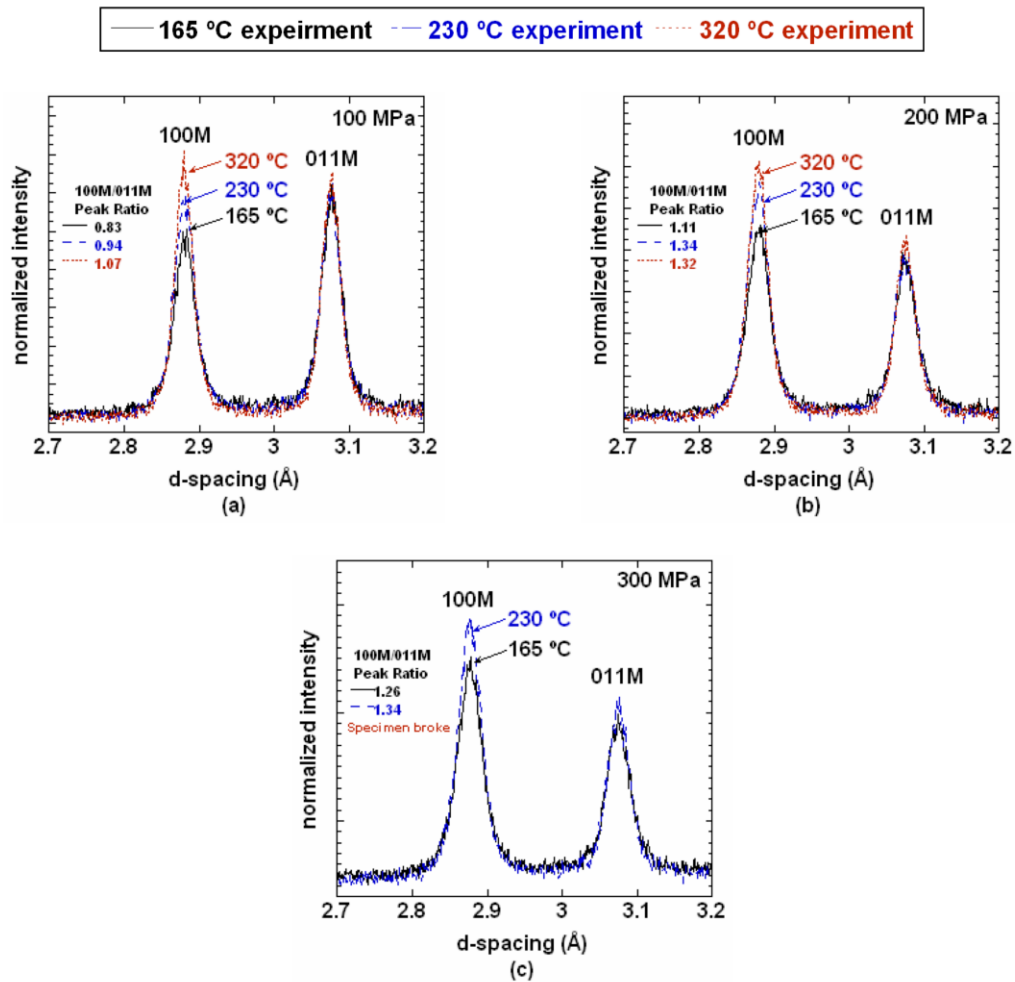

Figure 7: Section of normalized neutron diffraction spectra recorded at room temperature at different applied stresses of (a) 100 MPa, (b) 200 MPa and (c) 300 MPa showing the change in martensite texture, represented by ratios of the intensities of the 100 martensite reflections to the intensities of the 011 martensite reflections, with increasing upper-cycle temperature and stress. The spectra shown here are from diffracting lattice planes parallel to the loading axis.
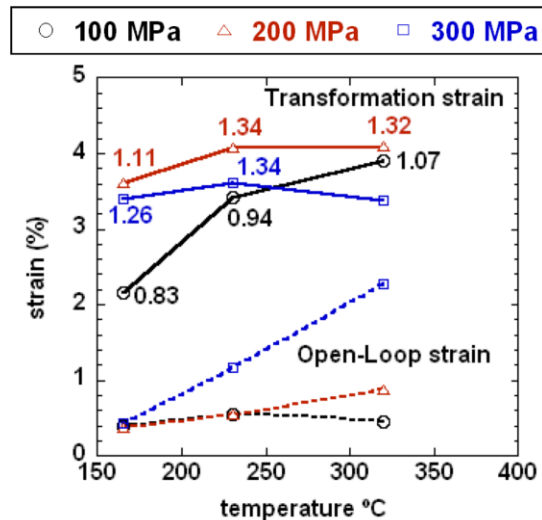
Figure 8: Correlation between texture evolution within the martensite phase and corresponding transformation and open-loop strains. Numbers shown in the graph are ratios of the intensities of the 100 martensite reflections to the intensities of the 011 martensite reflections from diffracting lattice planes parallel to the loading axis.

This lowering of the transformation capability, in the presence of small to no measurable changes in the texture of martensite, is probably related to the corresponding increase in the open-loop character of the material. As can be seen in Figures 6 and 8, the open-loop character of NiTi at 100 and 200 MPa are very similar, thus the increase in martensite texture results directly in an increase in the amount of transformation strain observed. Upon increasing the applied stress to 300 MPa, a significant increase in the open-loop character was observed. This increase when coupled with the slowing of the texture evolution resulted in a lowering of the actuation potential. It is thought that the increase in open-loop strain response and subsequent lowering of transformation strain capability is related to increases in volume fraction of the retained martensite and small amounts of localized plasticity, both of which affect the amount of strain that can be recovered during subsequent thermal cycles.

D.2 Evolution in Austenite

While the texture evolution that occurs within the martensite plays a major role in the observed actuator specific properties, it is equally important to investigate if there is any change occurring within the austenite, as the nature of the martensite and austenite phases dictate the character of the strain changes that will be observed. As previously shown, the increase in strain developed in the martensite was directly linked to the texture evolution occurring due to the stress and temperature employed during thermal cycling. Thus, increased strain in the martensite is tied to the volume fraction and orientation of the variants present. This is analogous to the strain increases that have been predicted to occur with changes in martensite volume fraction for the stress-induced case by Oliver *et al.* [17]. The reason for the increases in the absolute strains observed in the austenite with thermal cycling (which in this case were on the order of 5-15% as demonstrated in Figure 3) are not fully clear. While some of it can be explained as arising from retained martensite that co-exists with austenite, the role of other inelastic deformation mechanisms such as plasticity can also be a contributing factor.

The evolution of the austenite texture, when austenite co-exists with martensite, has previously been investigated by Bourke and Vaidyanathan [18-19]. To determine if retained martensite could contribute to the austenite texture observations, neutron diffraction information was collected at temperatures above the A_f where the system would generally be presumed to be "fully" austenitic.

Figure 9 shows 111 and 110 austenite peak reflections from portions of normalized neutron diffraction spectra recorded at different UCTs and stress. The changes in the ratio of the peak intensities are indicative of evolving texture in the austenite that can arise due to its coexistence with retained martensite [18-19]. As this volume fraction of retained martensite changes with UCT and stress so does the ratio of the intensity of the 111 austenite reflection to that of the 110 austenite reflection. Again, we note that the discussion presented here is based on representative austenite single peak intensities in order to provide qualitative insight into the role of UCT and stress on the transformation and open-loop strains. A more complete and detailed analysis of the texture evolution that is consistent with these observations from the 111 and 110 austenite reflections is presented in a companion article [16].

It is also important to note that a significant difference in the amount of peak broadening was observed between specimens cycled to 165 ^{o}C when compared to those cycled to higher temperatures. This is indicated in Figure 9 by the significant narrowing of the 111 and 110 austenite peaks as the temperature is increased at the same applied stress. Figure 10 shows the full width half maximum (FWHM) of 111 and 110 austenite peaks plotted as a function of UCT for various stresses. While this narrowing is expected and may normally be attributed to relaxation of intergranular mismatch stresses between grains with increasing temperature, resulting in a more homogenous strain distribution, we believe that the disappearance of retained martensite additionally contributes to this narrowing with increasing temperature by reducing mismatch stresses between the austenite and retained martensite. Other work on this same material [20] will show that performing multiple load-biased thermal cycles under a compressive stress of 150 MPa at 130 ^{o}C results in a buildup of retained martensite with cycling, which leads to a corresponding increase in the strain broadening of the austenite peaks.

In support of this idea, the diffraction data presented in Figure 11 for the 300 MPa/165 ^{o}C condition shows a 100 martensite peak providing direct evidence for the presence of retained martensite in the material. For this case, the volume fraction of retained martensite was determined to be roughly 3-4%. Thus the increased broadening at higher stresses is a result of the heterogeneous strain distribution arising from the higher applied external stresses themselves but also has contributions from the mismatch between retained martensite and austenite. It would be expected that the peak broadening observed for the 100 and 200 MPa conditions at 165 ^{o}C would also have contributions from the retained martensite albeit at levels less than that observed at 300 MPa, which would be below the detection limit of the neutron diffractometer.
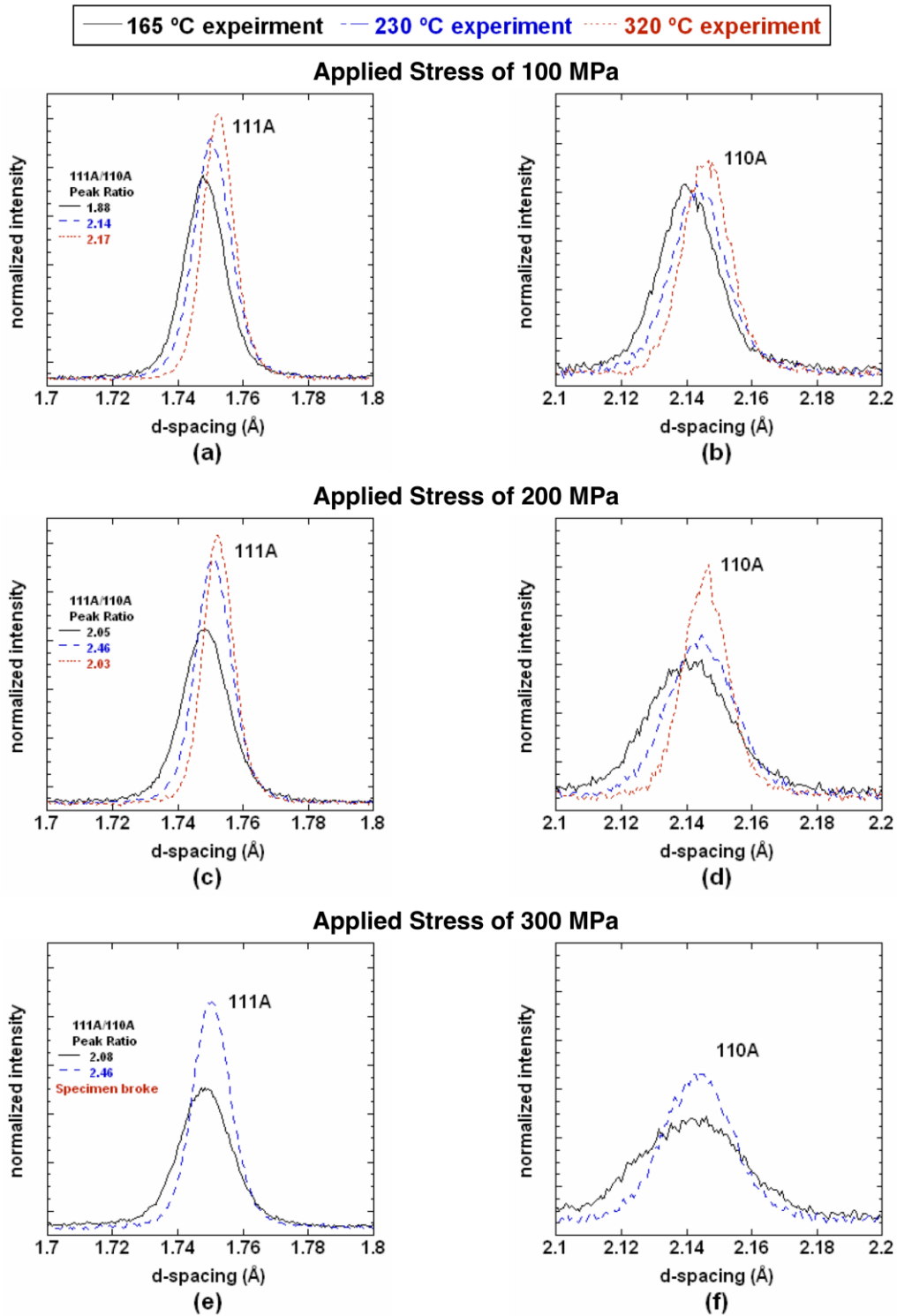
Figure 9: Section of normalized neutron diffraction spectra recorded in the austenite state at the respective upper-cycle temperatures for (a-b) 100 MPa, (c-d) 200 MPa and (e-f) 300 MPa, showing the change in internal strain and texture evolution, represented by peak intensity ratios of 111 austenite peak reflections to 110 austenite peak reflections, that develops with increasing upper-cycle temperature and stress. The spectra shown here are from diffracting lattice planes parallel to the loading axis.
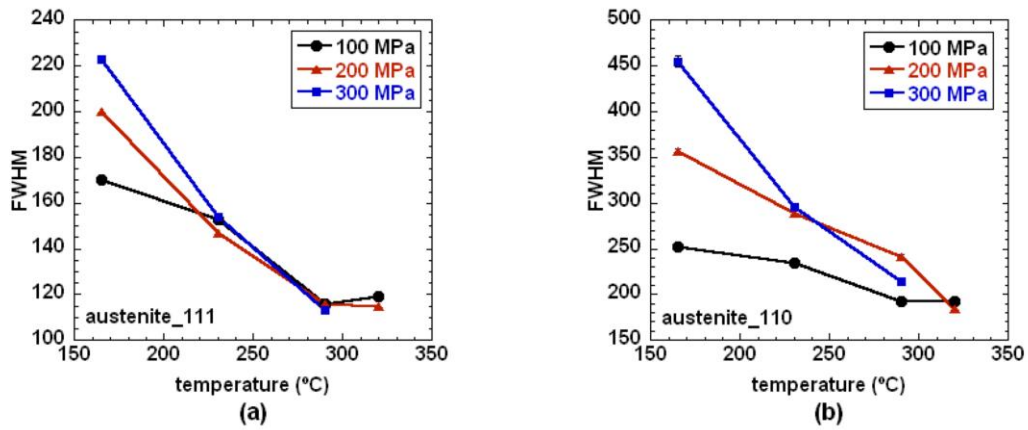
Figure 10: Changes in the full-width, half-maximum values for the 111 and 100 austenite peak reflections showing decreased broadening with increasing temperature and at lower UCTs, decreased broadening at lower stresses.
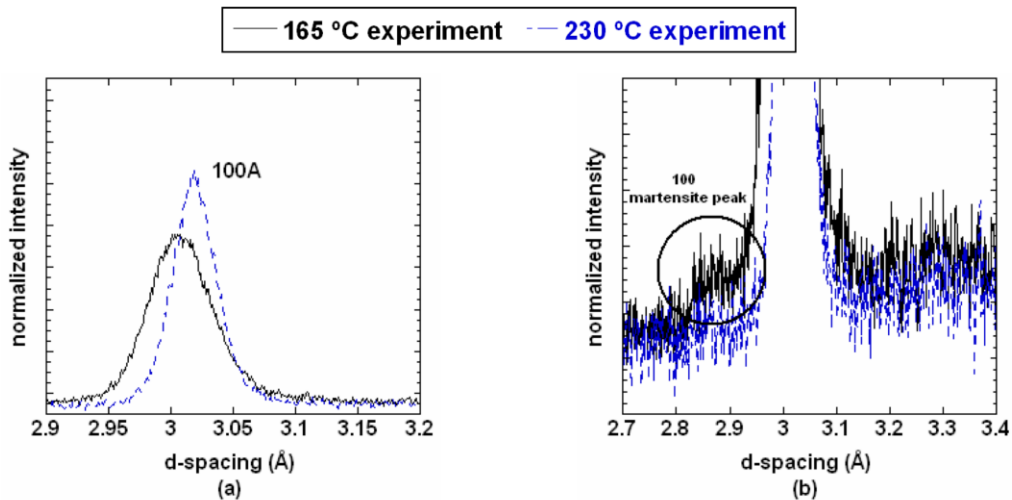

Figure 11: Neutron diffraction spectra taken in the austenite state at (a) 300 MPa showing significant strain broadening at 165 °C. (b) Magnified view of the spectra in (a) indicating the presence of retained martensite for the 300 MPa, 165 °C condition. The spectra shown here are from diffracting lattice planes parallel to the loading axis.

Peak broadening can also arise as a result of increases in the heterogeneity of the internal strain distribution resulting from plastic deformation. However, if increases in the amount of plasticity present in the material were responsible for the broadening, increased broadening would be expected with increases in the upper-cycle temperature since higher temperatures should decrease the flow stress of the material, thereby causing greater plasticity. This is not the case, making retained martensite effects the more likely operative mechanism responsible for the observed changes in internal strain, at least for

the temperature and stresses investigated. In reaching this conclusion we note that changes in broadening due to temperature are not significant as noted by careful examination of comparable spectra at different temperatures.

D.3 Overview of the Deformation Response

The impact of the applied stress and upper-cycle temperature on the overall observed behavior will now be illustrated in more detail using specific results from the current set of experiments. Starting with the 100 MPa/165°C condition, the transformation strain is relatively low because of the relatively weak 100 martensite texture and possible presence of retained martensite. However, as the applied stress is increased to 200 MPa at 165 ^{o}C, the texture evolves to a greater extent with a greater fraction of 100 variants aligned along the loading direction, thereby producing a greater amount of strain recovery. However, the amount of retained martensite can also be expected to increase. The results indicate that the change in the martensite texture at the higher stress overshadows the reduction in strain recovery that results from the higher levels of retained martensite at this stress. The result is a net transformation strain that is almost a factor of two larger for the 200 MPa condition when compared to 100 MPa at 165 ^{o}C. However, upon increasing the stress to 300 MPa, a different result is observed. In this case, the combination of a small increase in the strain potential due to the slight change in further evolution of the martensite texture with a greater amount of retained martensite, and hence lower amount of converted material, led to an overall transformation strain that is lower than was observed for the 200 MPa condition, albeit not by much at this temperature.

As the upper-cycle temperature was increased to 230 ^{o}C, stronger 100 texture in the martensite was observed compared to 165 ^{o}C for all stress levels tested (Figure 8). This indicates that the higher upper-cycle temperature produces a condition that favors preferred 100 variant formation along the loading direction of the sample, thereby increasing the strain recovery potential of the material. Although going to higher temperature reduced the amount of retained martensite, some texturing of the austenite phase was also observed. As mentioned earlier, this texturing of the austenite phase is required to accommodate the highly textured, but very small volume fraction of retained martensite given the correspondence between austenite and martensite. When all of these factors are combined, the net result is a higher transformation strain than was observed at 165 ^{o}C.

Similar arguments for the observed increases in transformation strain with increasing upper-cycle temperature can be made for temperatures up to 290 ^{o}C, where the transformation strain is maximized. Beyond this temperature, the levels of transformation strain were observed to decrease. As can be seen from the neutron diffraction information, the texture of the martensite phase reaches a maximum (for the peaks analyzed but also in a complete Rietveld analysis [16]) near the 290 ^{o}C condition. Beyond that, no additional strain potential would be expected for this material.

IV. Summary & Conclusions

The effects of stress and upper cycle temperature on the load-biased, shape memory behavior observed in this study can be rationalized by their effects on two opposing features. First, transformation strain is increased by factors that promote the development of texture in the martensite. In this work, the preferred martensite texture observed consisted of 100 variants aligned along the loading direction, which corresponds to a (11-1) type I twinned structure. In general, higher stresses and higher UCT tend to increase this observed martensite texture during the cooling portion of the thermal cycle, up to certain limits. In terms of applied stress, there appears to be a critical stress beyond which the observed martensite texture at cycle 2 appears to reach a maximum. This was about 200 MPa in the current set of experiments. Similarly, texture appears to reach a maximum at UCTs above about $230^{\circ}C$, which is roughly $110^{\circ}C$ above the nominal A_f.

Second, transformation strain is limited by factors that promote retained martensite during the heating cycle, at temperatures above the nominal A_f. Although these observations were drawn based on the behavior at cycle 2, it is believed that this information was sufficient to expose the key features and mechanisms responsible for strain evolution and changes in shape memory behavior early on during thermal cycling, where the largest changes are observed. It was noted that very small volume fractions of retained martensite, on the order of 3 vol. % or less, resulted in an austenite texture change and a corresponding decrease in transformation strain. In general, higher temperatures and lower stresses tended to produce less retained martensite upon heating while stresses above 200 MPa decreased the transformation strain because they result in increased retained martensite. Increases in UCT also eventually lead to a maximum in transformation strain, although the mechanisms responsible for the reductions in transformation strain above the maximum are not yet fully clear.

Finally, the measured transformation temperatures were observed to vary significantly with changes in both applied stress and upper-cycle temperature. Curiously, the slope of the temperature vs. applied stress plot $(dT/d\sigma)$ and the absolute value of the transformation temperature observed varied significantly, depending on the upper-cycle temperature used in the experiment. Reasons for the nature of this observation are not entirely clear and a detailed investigation is warranted.

References

1. S.A. Padula II, D.J. Gaydosh, R.D. Noebe, G.S. Bigelow, A. Garg, D. Lagoudas, I. Karaman, and K.C. Atli: *Behavior and Mechanics of Multifunctional and Composite Materials II*, SPIE Conf. Proc., 2008, vol. 6929, pp. 692912-1 to 692912-11.

2. X.D. Wu, G.J. Sun, and J.S. Wu: *Mater. Lett.*, 2003, vol. 57, pp. 1334-1338.

3. B. Ye, B.S. Majumdar, and I. Dutta: *Acta Mater.*, 2009, vol. 57, pp. 2403-2417.

4. J.H. Mabe, R. Ruggeri, and F.T. Calkins: *Proceedings of the International Conference on Shape Memory and Superelastic Technologies (SMST)*, 2006, pp. 629-644.

5. G.S. Bigelow, R.D. Noebe, S.A. Padula, and A. Garg: *Proceedings of the International Conference on Shape Memory and Superelastic Technologies (SMST)*, 2006, pp. 113-131.

6. R.D. Noebe, S.L. Draper, D.J. Gaydosh, A. Garg, B. Lerch, N. Penney, G.S. Bigelow, and S.A. Padula: *Proceedings of the International Conference on Shape Memory and Superelastic Technologies (SMST)*, 2006, pp. 409-426.

7. L.L. Toia, A. Coda, G. Vergani, L. Fumagalli, and F. Butera: *Proceedings of the International Conference on Shape Memory and Superelastic Technologies (SMST)*, 2006, pp. 499-506.

8. H. Warlimont, L. Delaey, R.V. Krisknan, and H. Tas: *J. Mater. Sci.*, 1974, vol. 9, pp. 1545-1555.

9. K.N. Melton and O. Mercier: *Acta Metall.*, 1981, vol. 29, pgs. 393-398.

10. A. Stebner, S. Padula II, R. Noebe, B. Lerch, and D. Quinn: *J. Intell. Mater. Syst. Struct.*, 2009, vol. 20, pp. 2107-2126.

11. M.A.M. Bourke, D.C. Dunand, and E. Ustundag: *Appl. Phys. A*, 2002, vol. 74, S1707.

12. R. Vaidyanathan, M.A.M. Bourke, and D.C. Dunand: *Metall. Mater. Trans. A*, 2001, vol. 32, pp.777-86.

13. S. Qiu, V.B. Krishnan, S.A. Padula II, R.D. Noebe, D.W. Brown, B. Clausen, and R. Vaidyanathan: *Appl. Phys. Lett.,* 2009, vol. 95, 141906.

14. S. Rajagopalan, A.L. Little, M.A.M. Bourke, and R. Vaidyanathan, *Appl. Phys. Lett.,* 2005, vol. 86, 081901.

15. D.C. Dunand, D. Mari, M.A.M Bourke, and J.A. Roberts: *Metall. Mater. Trans. A,* 1996, vol. 27, pp. 2820-36.

16. S. Qiu, S.A. Padula II, R.D. Noebe, D.W. Brown, and R. Vaidyanathan: *Metall. Mater. Trans. A* (to be submitted)

17. E.C. Oliver, N. Kobayashi, T. Mori, M.R. Daymond, and P.J. Withers: *Scr. Mater.*, 2003, vol. 49, pp. 1013-1019.

18. M.A.M. Bourke, R. Vaidyanathan, and D.C. Dunand: *Appl. Phys. Lett.*, 1996, vol. 69, pp. 2477-79.

19. R. Vaidyanathan, M.A.M. Bourke, and D.C. Dunand: *J. Appl. Phys.*, 1999, vol. 86, pp. 3020-29.

20. S. Qiu, S.A. Padula II, R.D. Noebe, and R. Vaidyanathan: *Acta Mater.* (to be submitted)

1. REPORT DATE (DD-MM-YYYY) 01-12-2011	2. REPORT TYPE Technical Memorandum	3. DATES COVERED (From - To)

4. TITLE AND SUBTITLE Effect of Upper-Cycle Temperature on the Load-Biased, Strain-Temperature Response of NiTi	5a. CONTRACT NUMBER
	5b. GRANT NUMBER
	5c. PROGRAM ELEMENT NUMBER
6. AUTHOR(S) Padula, Santo, II; Noebe, Ronald; Bigelow, Glen; Qiu, Shipeng; Vaidyanathan, Raj; Gaydosh, Darrell; Garg, Anita	5d. PROJECT NUMBER
	5e. TASK NUMBER
	5f. WORK UNIT NUMBER WBS 561581.02.08.03.43.04.01

7. PERFORMING ORGANIZATION NAME(S) AND ADDRESS(ES) National Aeronautics and Space Administration John H. Glenn Research Center at Lewis Field Cleveland, Ohio 44135-3191	8. PERFORMING ORGANIZATION REPORT NUMBER E-18055

9. SPONSORING/MONITORING AGENCY NAME(S) AND ADDRESS(ES) National Aeronautics and Space Administration Washington, DC 20546-0001	10. SPONSORING/MONITOR'S ACRONYM(S) NASA
	11. SPONSORING/MONITORING REPORT NUMBER NASA/TM-2011-217408

12. DISTRIBUTION/AVAILABILITY STATEMENT
Unclassified-Unlimited Subject Category: 26 Available electronically at http://www.sti.nasa.gov This publication is available from the NASA Center for AeroSpace Information, 443-757-5802

13. SUPPLEMENTARY NOTES

14. ABSTRACT
Over the past decade, interest in shape memory alloy based actuators has increased as the primary benefits of these solid-state devices have become more apparent. However, much is still unknown about the characteristic behavior of these materials when used in actuator applications. Recently we have shown that the maximum temperature reached during thermal cycling under isobaric conditions could significantly affect the observed mechanical response of NiTi (55 wt% Ni), especially the amount of transformation strain available for actuation and thus work output. The investigation we report here extends that original work to ascertain whether further increases in the upper-cycle temperature would produce additional changes in the work output of the material, which has a stress-free austenite finish temperature of 113 °C, and to determine the optimum cyclic conditions. Thus, isobaric, thermal-cycle experiments were conducted on the aforementioned alloy at various stresses from 50-300 MPa using upper-cycle temperatures of 165, 200, 230, 260, 290, 320 and 350 °C. The data indicated that the amount of applied stress influenced the transformation strain, as would be expected. However, the maximum temperature reached during the thermal excursion also plays an equally significant role in determining the transformation strain, with the maximum transformation strain observed during thermal cycling to 290 °C. In situ neutron diffraction at stress and temperature showed that the differences in transformation strain were mostly related to changes in martensite texture when cycling to different upper-cycle temperatures. Hence, understanding this effect is important to optimizing the operation of SMA-based actuators and could lead to new methods for processing and training shape memory alloys for optimal performance.

15. SUBJECT TERMS
Shape memory alloy; NiTi; Thermomechanical behavior; Actuator; Standards

16. SECURITY CLASSIFICATION OF:			17. LIMITATION OF ABSTRACT	18. NUMBER OF PAGES	19a. NAME OF RESPONSIBLE PERSON STI Help Desk (email:help@sti.nasa.gov)
a. REPORT U	b. ABSTRACT U	c. THIS PAGE U	UU	25	19b. TELEPHONE NUMBER (include area code) 443-757-5802